

## Experimental characterization of Gaussian quantum discord generated by four-wave mixing

Ulrich Vogl,<sup>\*</sup> Ryan T. Glasser, Quentin Glorieux, Jeremy B. Clark, Neil V. Corzo, and Paul D. Lett

*Quantum Measurement Division, National Institute of Standards and Technology and Joint Quantum Institute, NIST and the University of Maryland, Gaithersburg, Maryland 20899, USA*

(Received 5 August 2012; published 16 January 2013)

We experimentally determine the Gaussian quantum discord present in two-mode squeezed vacuum generated by a four-wave mixing process in hot rubidium vapor. The frequency spectra of the discord as well as the quantum and classical mutual information are also measured. In addition, the effects of symmetric attenuation introduced into both modes of the squeezed vacuum on the Gaussian quantum discord, and the quantum mutual information and the classical correlations are examined experimentally. Finally, we show that due to the multi-spatial-mode nature of the four-wave mixing process, the Gaussian quantum discord may exhibit sub- or superadditivity depending on which spatial channels are selected.

DOI: [10.1103/PhysRevA.87.010101](https://doi.org/10.1103/PhysRevA.87.010101)

PACS number(s): 03.65.Ud, 42.50.Ex, 42.50.Lc

Quantum communication and computation schemes have been thought to rely necessarily on entanglement to offer improvements over classical systems. While entangled systems have certainly been shown to provide enhancements beyond classical boundaries, it may be beneficial in some cases to consider more general measures of quantum correlations. More recently, a different measure of the degree of quantumness of correlations that a bipartite system contains has been proposed: the quantum discord, which allows an appropriate characterization of the quantumness of mixed states [1–7]. This quantity is defined as the difference between two classically equivalent expressions for the mutual information, when applied to a quantum system. It has since been suggested that systems that are not entangled, but exhibit nonzero quantum discord, still may allow for quantum enhancements in a variety of situations [8–10].

While it is still unclear that the quantum discord can strictly be identified as the resource allowing particular quantum advantages, these results are suggestive that quantum discord is, in some scenarios, a more faithful measure of nonclassicality, as it is sensitive to correlations that are ignored by measures like the inseparability or the logarithmic negativity [5,6]. The concept of quantum discord may also stimulate new approaches in continuous variable quantum information [11] with Gaussian states [12], and possibly beyond the Gaussian regime [13,14].

Despite the rapidly growing body of theoretical works concerning quantum discord, few experiments have investigated the topic [15–20]. This may be partly due to the fact that analytic procedures to determine discord in experimental systems involving mixed states are not yet as established as for pure states. Here we measure the amount of Gaussian quantum discord, as well as quantum mutual information and classical mutual information, that are present in twin beams created by the vacuum-seeded four-wave mixing (4WM) process in hot Rb vapor. This is based on experimental reconstruction of the covariance matrix of the system. Additionally, we demonstrate the relative robustness of discord as a nonclassicality measure, as evidenced by the fact that even for vanishing squeezing,

nonzero quantum discord still exists. Zero Gaussian quantum discord is reached only for product states (i.e., classical states) [3]. Finally, we show that the multi-spatial-mode nature of 4WM results in dramatically different behavior of the discord depending on which pairs of spatial subchannels of the system are used.

We begin by summarizing the concept of mutual information as applied to both classical and quantum systems and introduce the concept of quantum discord. Classical information theory results in two equivalent expressions for the mutual information present in a bipartite system with two random variables  $A$  and  $B$ , which take on the values  $a$  and  $b$ , with the probabilities  $p_A(a)$  and  $p_B(b)$ , respectively. The joint probability  $p_{AB}(a,b)$  of the system characterizes the correlations between the systems  $A$ ,  $B$ . The two alternative formulations for the classical mutual information are [1]

$$I_M(A:B) = H(A) + H(B) - H(A,B) \quad \text{and} \\ J(A:B) = H(B) - H(B|A). \quad (1)$$

Here  $H(X) = -\sum p(x) \log_2 p(x)$  is the marginal entropy of the probability distribution for a given result  $X$ ,  $H(A,B)$  is the joint marginal entropy, and  $H(B|A)$  is the conditional entropy, describing the average entropies of  $B$  conditioned on the alternative outcomes of  $A$  following Bayes's rule. Equation (1) determines the amount of information one can gain about subsystem  $A$  upon measurement of subsystem  $B$ . Quantum discord results from the fact that the two classical formulations of mutual information generally do not coincide for a state represented by the density matrix  $\rho_{AB}$ . In the quantum case, the marginal entropy is replaced by the von Neumann entropy  $S(\rho) = -\text{Tr}(\rho \log_2 \rho)$  and yields

$$I_M(\rho_{AB}) = S(\rho_A) + S(\rho_B) - S(\rho_{AB}). \quad (2)$$

The expression for  $J(A:B)$  contains the conditional entropy  $H(B|A)$ , which, when applied to the quantum case, results in a term that requires minimization over all possible measurements on subsystem  $A$  (due to the ambiguity in defining the state of subsystem  $B$  before measuring subsystem  $A$ ). In general, for the quantum case  $I_M \neq J$ , as here measurements on only one subsystem do not give full knowledge about all of the existing correlations. The difference is the discord

<sup>\*</sup>ulrich.vogl@nist.gov

$D = I_M - J$ , given by

$$\mathcal{D}(A; B) = H(\rho_A) - H(\rho_B) + \inf_{A_k} \sum_k p_{A_k} H(\rho_{B|k}), \quad (3)$$

where the infimum describes the optimization over all possible measurements performed on system  $A$ . This necessary optimization makes it an open problem to find an applicable expression for this term under many experimental situations.

To calculate the quantum discord present in a given system assumptions about the state of the system must be made. We now concentrate on the special case of discord for two-mode Gaussian states, for which an analytic solution has been given in Ref. [5] and, specifically for symmetric squeezed thermal states, in Ref. [21]. The formalism requires knowledge of the covariance matrix of the bipartite state. In the following we show explicitly how to derive the Gaussian quantum discord from experimentally obtainable data, based on the theoretical description of Adesso and Datta [5].

A two-mode Gaussian state  $\rho_{AB}$  can be described by its covariance matrix  $\gamma_{AB}$ , which may be transformed into the standard form [22,23] with diagonal subblocks

$$\gamma_{AB} = \begin{pmatrix} n & 0 & c_1 & 0 \\ 0 & n & 0 & c_2 \\ c_1 & 0 & m & 0 \\ 0 & c_2 & 0 & m \end{pmatrix}, \quad (4)$$

with the symplectic invariants  $I_1 = n^2$ ,  $I_2 = m^2$ ,  $I_3 = c_1 c_2$ , and  $I_4 = (nm - c_1^2)(nm - c_2^2)$  and symplectic eigenvalues

$$d_{\pm} = \sqrt{\frac{\Delta \pm \sqrt{\Delta^2 - 4I_4}}{2}}, \quad (5)$$

where  $\Delta = I_1 + I_2 + 2I_3$ .

The values  $n, m, c_1$ , and  $c_2$  are experimentally accessible via homodyne and joint-homodyne measurements, as discussed in the following. This allows one to express the quantum mutual information, the classical correlations, and the Gaussian quantum discord as a function of the symplectic invariants [5]:

$$I_M = h(\sqrt{I_1}) + h(\sqrt{I_2}) - h(d_+) - h(d_-), \quad (6)$$

$$J = h(\sqrt{I_1}) - h(\sqrt{E_{A|B}^{\min}}), \quad (7)$$

$$\mathcal{D}_{A;B}(\gamma_{AB}) = h(\sqrt{I_2}) - h(d_-) - h(d_+) + h(\sqrt{E_{A|B}^{\min}}) \quad (8)$$

with

$$E_{A|B}^{\min} = \begin{cases} \frac{2I_3^2 - (I_1 - 4I_4)(I_2 - \frac{1}{4}) + 2|I_3| \sqrt{I_3^2 - (I_1 - 4I_4)(I_2 - \frac{1}{4})}}{4(I_2 - \frac{1}{4})^2} & \text{if } \frac{(I_1 I_2 - I_4)^2}{(I_1 + 4I_4)(I_2 + \frac{1}{4})I_3^2} \leq 1, \\ \frac{I_1 I_2 - I_3^2 + I_4 - \sqrt{I_3^4 + (I_1 I_2 - I_4)^2 - 2I_3^2(I_1 I_2 + I_4)}}{2I_2} & \text{otherwise,} \end{cases} \quad (9)$$

where  $h(x) = (x + \frac{1}{2}) \log_2(x + \frac{1}{2}) - (x - \frac{1}{2}) \log_2(x - \frac{1}{2})$ .  $\mathcal{D} > 1$  is a sufficient condition for demonstrating the entanglement of Gaussian states, and  $\mathcal{D} = 0$  is reached for classical states. A condition arising from the uncertainty relation requires  $d_- \geq 1/2$  in order for a state to be physical [5].

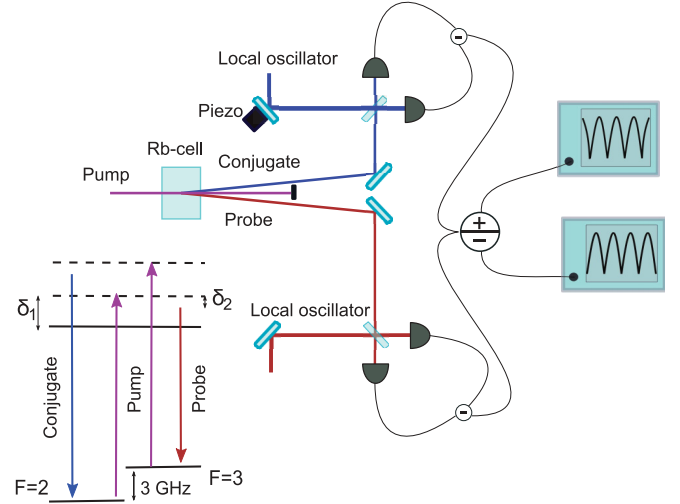


FIG. 1. (Color online) Experimental setup for determining the elements of the covariance matrix. Two-mode squeezed vacuum is generated by a 4WM process. Probe and conjugate beams are generated in a cone around the pump beam with an angle  $\approx 1^\circ$ . Each beam is separately overlapped with a strong local oscillator beam on a 50:50 beam splitter, where both outputs are fed into a photodetector. The relative phase of the local oscillators is scanned by a piezo mirror in one path. The sum and difference of the generated photocurrent signals are fed into electronic spectrum analyzers.  $\delta_1$  and  $\delta_2$  are the one- and two-photon detunings, respectively.

The formulation of Gaussian quantum discord in Eqs. (8) and (9) allows for direct experimental access via homodyne and dual-homodyne detection [24–27]. A two-mode squeezed vacuum is generated in multiple spatial modes by a 4WM process near the  $^{85}\text{Rb}$   $D_1$  line  $|5S_{1/2}, F=2\rangle \rightarrow |5P_{1/2}\rangle$ , at  $\lambda \approx 795$  nm as described in Ref. [28] and indicated in Fig. 1; probe and conjugate modes are generated at  $\pm 3$  GHz relative to the pump. The one-photon detuning is  $\delta_1 \approx 800$  MHz, and the two-photon detuning  $\delta_2$  is effectively 0 MHz, as the detected field is determined by the local oscillator detuning. Bright local oscillator beams are created by seeding a second 4WM process that has otherwise the same experimental parameters as the first 4WM process, as in Ref. [28].

The case examined here involves a symmetric two-mode squeezed state which allows for a simple treatment, resulting in direct experimental access to the nonzero matrix elements in Eq. (4). A single homodyne detection of each of the modes  $A$  and  $B$  gives the excess noise fluctuations of the individual modes

$$\Delta^2 X_A \quad \text{and} \quad \Delta^2 X_B, \quad (10)$$

which, when scaled by the shot-noise limit (SNL), results in the matrix elements  $n$  and  $m$ , respectively. The off-diagonal matrix elements  $c_1$  and  $c_2$  are extracted from measurements of the fluctuations of the joint-amplitude and phase quadratures (difference and sum, respectively):

$$X_- = (X_A - X_B)/\sqrt{2}, \quad Y_+ = (Y_A + Y_B)/\sqrt{2}. \quad (11)$$

Here  $X_A, X_B$  and  $Y_A, Y_B$  are the amplitude and phase quadratures of states  $A$  and  $B$ , respectively. Experimentally, this corresponds to two separate measurements of the sum and difference signals of a joint-homodyne detection of both

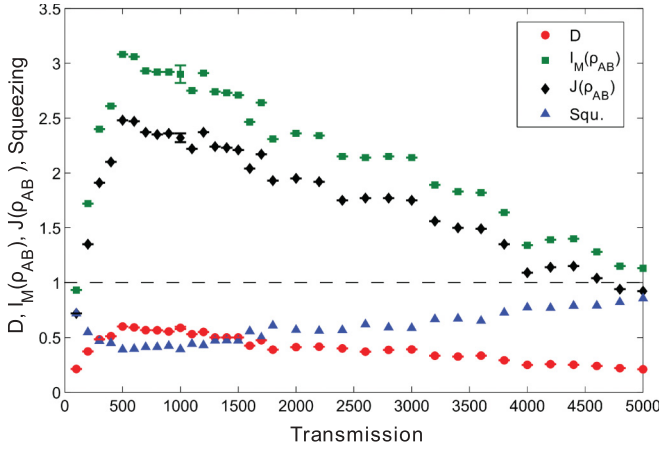


FIG. 2. (Color online) Frequency spectrum for the extracted Gaussian quantum discord (red circles), quantum mutual information  $I_M(\rho_{AB})$  (green squares), classical correlations  $J(\rho_{AB})$  (black diamonds), and squeezing (blue triangles), respectively (the shot noise limit is indicated with a dashed line). These measurements, taken at different RF center frequencies shown, serve to vary the off-diagonal covariance matrix elements (that depend on the amount of squeezing), while effectively keeping the on-diagonal elements constant (these depend only on the excess noise in each single mode).

modes, while scanning the path length of one of the local oscillators relative to the other, as indicated in Fig. 1. These photocurrents give direct access to the variances of the two joint quadratures  $\Delta^2 X_-$  and  $\Delta^2 Y_+$  when the local oscillator is scanned and the trace reaches a minimum. We can then directly determine the off-diagonal entries of the covariance matrix

$$c_1 = \Delta^2 X_A - \Delta^2 X_- \quad \text{and} \quad c_2 = \Delta^2 Y_B - \Delta^2 Y_+, \quad (12)$$

after normalizing each quantity to the SNL.

We experimentally examine the frequency spectrum of the Gaussian quantum discord in our system by changing the RF center frequency at which the measurements are made. The joint quadrature squeezing and the excess noise on the individual probe and conjugate beams are expected to exhibit a somewhat different frequency dependence due to the variation of the extra noise from the 4WM process. The measured spectra of discord,  $I_M$ ,  $J$ , and squeezing are shown in Fig. 2. The noise variance (blue triangles), normalized such that 1 corresponds to the SNL and 0 is perfect squeezing, exhibits excess noise at low frequencies due to technical noise. Optimum squeezing is obtained in the range  $\approx 500$  kHz to 1 MHz, with decreasing measured squeezing at higher detection frequencies. (All uncertainties shown are one standard deviation, combined statistical and systematic uncertainties. The statistical uncertainty is obtained from the variance on the measured shot noise and excess noise on the single beam measurements and the joint quadrature measurements. In Fig. 2 the uncertainties are shown at only one frequency, but are representative of typical uncertainties.) Though not shown in the plot, there exists nonzero discord for some distance after squeezing has reached zero. The frequency spectrum of the squeezing is largely reflected in the spectra of the discord (red dots), the quantum mutual information (green squares), and the classical correlations (black diamonds),

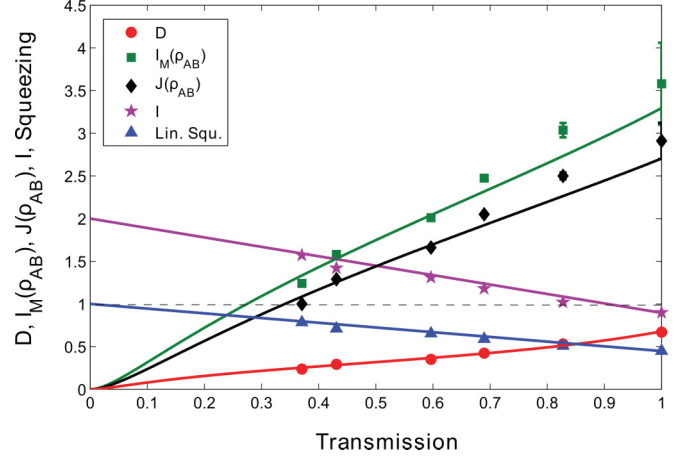


FIG. 3. (Color online) Gaussian quantum discord (red circles), inseparability  $I$  (purple stars), quantum mutual information  $I_M(\rho_{AB})$  (green squares), classical correlations  $J(\rho_{AB})$  (black diamonds), and squeezing (blue triangles, plotted on a linear scale) versus the (symmetric) transmission of each two-mode squeezed vacuum path when attenuated with neutral density filters.  $I$  at each point is  $< 2$ , confirming that the state is inseparable. The theory curves are calculated by using the measured initial squeezing and excess noise at a transmission of one.

showing that each of these measures are equally good for investigating the qualitative variation of bipartite correlations.

The Gaussian quantum discord captures information about all of the elements of the covariance matrix. Another measure, the inseparability criterion, defined as  $I = \langle \Delta X_-^2 \rangle + \langle \Delta Y_+^2 \rangle$ , contains information only about the off-diagonal elements. We now examine how the discord,  $I_M$ ,  $J$ , and  $I$  scale with the symmetric attenuation of the two-mode squeezed vacuum state. Before the double-homodyne measurement, we symmetrically vary the amount of attenuation in both modes of the two-mode squeezed vacuum state with a neutral density filter. This serves to change all of the elements of the derived covariance matrix in a controllable, symmetric manner. In Fig. 3 we plot the quantum discord (red dots), the inseparability (purple stars),  $I_M$ , and  $J$  versus the transmission of the state, where we attenuate both beams identically with neutral density filters. The state is inseparable for all values of transmission measured, according to the criterion of  $I < 2$ . The discord,  $I_M$ , and  $J$  are all monotonically increasing functions of transmission and diverge from one another as the transmission is increased. The theoretical curves in Fig. 3 are calculated for varying attenuation (with the standard beam splitter model for losses [29]) at a transmission of one, with no free parameters. While the inseparability and the squeezing (blue triangles) show linear behavior versus attenuation, the discord curve is slightly nonlinear, indicating the influence of the on-diagonal elements of Eq. (4).

Squeezing and entanglement in multi-spatial-mode states have been shown to allow for enhanced resolution in imaging and for the possibility of spatial multiplexing (cf. Ref. [30], and the role of classical and quantum correlations in imaging has been emphasized [31]. The present 4WM system can exhibit multi-spatial-mode twin-beam correlations between the probe and conjugate beams [32]. An adequate analytic description

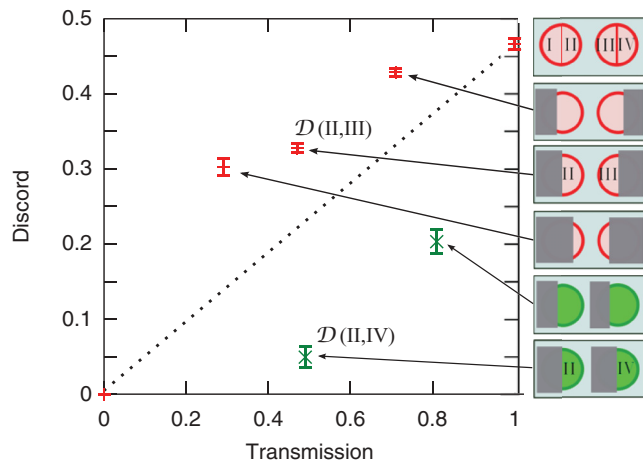


FIG. 4. (Color online) Gaussian quantum discord as a function of transmission of the local oscillator beams. The local oscillator beams were clipped symmetrically (red crosses) and antisymmetrically (green stars) as sketched on the right. The points for  $\approx 50\%$  clipping are indicated, and the insets have the subregions for 50% clipping labeled with Roman numerals.

of the generated multi-spatial-mode states suffers often from poor knowledge of the appropriate basis [33], which is usually worsened by the admixture of thermal photons. The spatial distribution of the quantum correlations represented by the Gaussian quantum discord may here give a better insight to what extent different subareas of the generated beams can be used as independent channels for quantum information processing.

We now investigate the discord and quantum mutual information that is present between various bimodal subchannels of the two-mode squeezed vacuum. Our aim is to investigate in this context the subadditivity of information measures and channel capacity [34,35], which in our case result directly from the multi-spatial-mode nature of the Gaussian quantum discord. Subadditivity of a channel is defined here as the situation when the discord of the total bipartite channel is smaller than the sum of the discord between two bipartite subchannels. Superadditivity is then the converse. Let us define four channels, made up of combinations of one of the regions I and II as the left and right halves of the probe mode, and one of the regions III and IV as the left and right halves of the conjugate mode (as shown in Fig. 4). The correlations between spatial regions in the probe mode and the conjugate mode are expected to be centro-symmetric with respect to the pump beam, as indicated in Fig. 1, which allows us to differentiate between mostly correlated and largely uncorrelated subregions.

We measure the Gaussian quantum discord,  $\mathcal{D}(\text{II};\text{IV})$ , present between modes II and IV by cutting the local oscillator beams with a knife edge, and allowing only these modes to be fed into the dual-homodyne detection system. This serves to project out only modes II and IV. As seen in Fig. 4, the quantum

discord present between these two channels,  $\mathcal{D}(\text{II};\text{IV})$ , is much less than half of the total discord present between the entire, uncut probe and conjugate modes,  $\mathcal{D}(\text{I} + \text{II}; \text{III} + \text{IV})$ . In this case, the discord is superadditive, or in other words, we have chosen subregions of the beams that are largely uncorrelated. The same result is obtained with  $\mathcal{D}(\text{I};\text{III})$ , confirming the spatial symmetry when clipping the beams in this direction. In contrast, the discord between modes II and III,  $\mathcal{D}(\text{II};\text{III})$ , is significantly more than half of the total discord between the total, uncut modes. In this scenario, the discord behaves subadditively. This subadditive property [34] of the discord may allow for more effectively exploiting the channel capacity of a total system if it is correctly divided into various bimodal subchannels [36]. This shows that the discord varies dramatically in multi-spatial-mode squeezed vacuum systems, depending on which spatial channels are utilized. Here, when symmetric channels are used, the discord is subadditive with respect to the unaltered system. We also find that when asymmetric channels are chosen, the amount of discord quickly decreases, resulting in superadditive behavior.

Existing theoretical work concerning quantum discord indicates that discord can in principle be employed in various quantum computation and quantum communication schemes to provide enhancements beyond those allowed classically. In particular, many schemes require optical delay and storage of quantum correlations that are always accompanied by some loss and decoherence. The relative robustness of quantum discord with respect to decoherence effects provides motivation to more closely investigate these systems experimentally. Specifically, the present scheme for the determination of Gaussian quantum discord is applicable if one is interested in the evolution of quantum correlations in systems that involve stored light [37] and fast light [38,39], where squeezing and entanglement may be easily degraded. Discord as a measure of quantum correlations in mixed bipartite states may offer a means to experimentally test the nonbroadcasting theorem for the class of quantum-correlated bipartite states as a simple example of mixed states [40,41] under fast-light conditions, and how classical and discordant states can be distinguished in this regime. Examining the amount of discord and comparing it with measures like squeezing or entanglement present under these exotic conditions should allow for a clearer view of any “quantumness” that is present in the system. Finally, future investigations that compare how various measures of nonclassicality, including discord, are affected by decoherence may provide insight into the role each measure plays in quantum information and communication schemes.

This work was supported by the Air Force Office of Scientific Research. Ulrich Vogl would like to thank the Alexander von Humboldt Foundation. R.T.G. was supported by a National Research Council Research Associateship Award at NIST.

- [1] H. Ollivier and W. H. Zurek, *Phys. Rev. Lett.* **88**, 017901 (2001).  
 [2] L. Henderson and V. Vedral, *J. Phys. A: Math. General* **34**, 6899 (2001).

- [3] A. Ferraro, L. Aolita, D. Cavalcanti, F. M. Cucchietti, and A. Acin, *Phys. Rev. A* **81**, 052318 (2010).  
 [4] B. Dakić, V. Vedral, and Č. Brukner, *Phys. Rev. Lett.* **105**, 190502 (2010).

- [5] G. Adesso and A. Datta, *Phys. Rev. Lett.* **105**, 030501 (2010).
- [6] K. Modi, H. Cable, M. Williamson, and V. Vedral, *Phys. Rev. X* **1**, 021022 (2011).
- [7] A. Streltsov, H. Kampermann, and D. Bruß, *Phys. Rev. Lett.* **106**, 160401 (2011).
- [8] B. P. Lanyon, M. Barbieri, M. P. Almeida, and A. G. White, *Phys. Rev. Lett.* **101**, 200501 (2008).
- [9] A. Datta and A. Shaji, *Int. J. Quantum. Inform.* **09**, 1787 (2011).
- [10] L. Wang, J. H. Huang, J. P. Dowling, and S. Y. Zhu, *Quant. Info. Proc.* **12**, 899 (2012).
- [11] S. L. Braunstein and P. van Loock, *Rev. Mod. Phys.* **77**, 513 (2005).
- [12] G. Adesso and F. Illuminati, *J. Phys. A: Math. Theor.* **40**, 7821 (2007).
- [13] F. Dell'Anno, S. De Siena, and F. Illuminati, *Phys. Rep.* **428**, 53 (2006).
- [14] R. Tatham, L. Mišta, Jr., G. Adesso, and N. Korolkova, *Phys. Rev. A* **85**, 022326 (2012).
- [15] M. A. Yurishchev, *Phys. Rev. B* **84**, 024418 (2011).
- [16] R. Auccaise, J. Maziero, L. C. Céleri, D. O. Soares-Pinto, E. R. deAzevedo, T. J. Bonagamba, R. S. Sarthour, I. S. Oliveira, and R. M. Serra, *Phys. Rev. Lett.* **107**, 070501 (2011).
- [17] G. Passante, O. Moussa, D. A. Trotter, and R. Laflamme, *Phys. Rev. A* **84**, 044302 (2011).
- [18] L. S. Madsen, A. Berni, M. Lassen, and U. L. Andersen, *Phys. Rev. Lett.* **109**, 030402 (2012).
- [19] M. Gu, H. M. Chrzanowski, S. M. Assad, T. Symul, K. Modi, T. C. Ralph, V. Vedral, and P. K. Lam, *Nature Phys.* **8**, 671 (2012).
- [20] R. Blandino, M. G. Genoni, J. Etesse, M. Barbieri, M. G. A. Paris, P. Grangier, and R. Tualle-Brouri, *Phys. Rev. Lett.* **109**, 180402 (2012).
- [21] P. Giorda and M. G. A. Paris, *Phys. Rev. Lett.* **105**, 020503 (2010).
- [22] L.-M. Duan, G. Giedke, J. I. Cirac, and P. Zoller, *Phys. Rev. Lett.* **84**, 2722 (2000).
- [23] C. Weedbrook, S. Pirandola, R. García-Patrón, N. J. Cerf, T. C. Ralph, J. H. Shapiro, and S. Lloyd, *Rev. Mod. Phys.* **84**, 621 (2012).
- [24] J. Wenger, A. Ourjoumtsev, R. Tualle-Brouri, and P. Grangier, *Eur. Phys. J. D* **32**, 391 (2005).
- [25] W. P. Bowen, R. Schnabel, P. K. Lam, and T. C. Ralph, *Phys. Rev. A* **69**, 012304 (2004).
- [26] J. Laurat, G. Keller, J. A. Oliveira-Huguenin, C. Fabre, T. Coudreau, A. Serafini, G. Adesso, and F. Illuminati, *J. Opt. B: Quant. Semiclassical Opt.* **7**, 577 (2005).
- [27] V. D'Auria, S. Fornaro, A. Porzio, S. Solimeno, S. Olivares, and M. G. A. Paris, *Phys. Scr.* **2010**, 014018 (2010).
- [28] A. M. Marino, R. C. Pooser, V. Boyer, and P. D. Lett, *Nature (London)* **457**, 859 (2009).
- [29] C. F. McCormick, A. M. Marino, V. Boyer, and P. D. Lett, *Phys. Rev. A* **78**, 043816 (2008).
- [30] M. Kolobov, *Rev. Mod. Phys.* **71**, 1539 (1999).
- [31] S. Ragy and G. Adesso, *Scientific Reports* **2**, 651 (2012).
- [32] V. Boyer, A. M. Marino, R. C. Pooser, and P. D. Lett, *Science* **321**, 544 (2008).
- [33] N. Treps, V. Delaubert, A. Maître, J. Courty, and C. Fabre, *Phys. Rev. A* **71**, 013820 (2005).
- [34] N. J. Cerf, *Phys. Rev. A* **57**, 3330 (1998).
- [35] A. S. Holevo and V. Giovannetti, *Rep. Prog. Phys.* **75**, 046001 (2012).
- [36] F. Fanchini, M. F. Cornelio, M. C. de Oliveira, and A. O. Caldeira, *Phys. Rev. A* **84**, 012313 (2011).
- [37] Q. Glorieux, J. B. Clark, A. M. Marino, Z. Zhou, and P. D. Lett, *Opt. Express* **20**, 12350 (2012).
- [38] R. T. Glasser, U. Vogl, and P. D. Lett, *Phys. Rev. Lett.* **108**, 173902 (2012).
- [39] U. Vogl, R. T. Glasser, and P. D. Lett, *Phys. Rev. A* **86**, 031806 (2012).
- [40] H. Barnum, C. M. Caves, C. A. Fuchs, R. Jozsa, and B. Schumacher, *Phys. Rev. Lett.* **76**, 2818 (1996).
- [41] H. Barnum, J. Barrett, M. Leifer, and A. Wilce, *Phys. Rev. Lett.* **99**, 240501 (2007).